CMS Physics Analysis Summary

Contact: cms-pag-conveners-exotica@cern.ch 2015/12/16

Search for SSM W′ production, in the lepton+MET final state at a center-of-mass energy of 13 TeV

The CMS Collaboration

Abstract

This note presents the search for new physics in events with an electron or muon and missing transverse energy, using 2.2 fb^{-1} of pp collision data at $\sqrt{s} = 13$ TeV, collected by the CMS detector during 2015. The focus is set on the potential production of a W′ boson, as described by the Sequential Standard Model (SSM). No evidence of an excess relative to the Standard Model expectation is observed and upper limits at 95% confidence level are set on the production cross section times branching fractions of the SSM W′ boson, which are translated into lower limits for the new boson mass. For a SSM W′ signal masses below 4.4 TeV are excluded when both the electron and muon final decay channels are combined together. These results significantly extend previously published limits.

1 Introduction

Many SM extensions predict additional heavy gauge bosons. In particular the Sequential Standard Model (SSM) [1] predicts the existence of a new massive boson, W′, exhibiting the same couplings as the Standard Model (SM) W boson, decaying in final states with a charged lepton and neutrino, or quark pairs. If sufficiently massive, the decay channel $W' \to t\bar{b}$ is also allowed.

The analysis presented in this paper addresses deviations from the SM prediction in events with a charged lepton (electron or muon) and one (or more) particles that cannot be directly detected (neutrino, dark matter particle) in the final state. In particular it allows the search for a W′ boson, where the decays to bosons (W, Z, H) are assumed to be suppressed. No interference with the W boson from the SM is considered.

Similar searches have been carried out at several past experiments and accelerators, finding no indication for any deviation in terms of new physics and setting lower limits to the mass of a potential SSM W′ boson. The most stringent limits up-to-date come from the LHC experiments, ATLAS [2] and CMS [3]. Current limits obtained by CMS with an integrated luminosity of $19.7 \pm 0.5\,\text{fb}^{-1}$ of proton-proton collisions at a center-of mass energy of 8 TeV, are 3.22 TeV in the electron channel, and 2.99 TeV in the muon one. Combining both channels results in an exclusion of W′ bosons with a mass less than 3.28 TeV. The ATLAS results at $\sqrt{s} = 8\,\text{TeV}$ exclude W′ bosons with masses less than 3.24 TeV.

Due to the increase in the center-of-mass energy from 8 to 13 TeV the parton luminosities associated to $q\bar{q}$ interactions (at the origin of W′ bosons) increase very substantially in the high mass region. This note presents the analysis of $2.2\,\text{fb}^{-1}$ of proton–proton collisions taken by the CMS detector during 2015, at a center-of mass energy of 13 TeV.

2 CMS Detector

A detailed description of the CMS detector and the coordinate system used can be found elsewhere [4]. The central feature of the CMS apparatus is a superconducting solenoid of 6 m internal diameter providing an axial field of 3.8 T. Within the field volume are located the silicon pixel and strip tracker ($|\eta| < 2.4$) and the barrel and endcap calorimeters ($|\eta| < 3$); a lead tungstate crystal electromagnetic calorimeter (ECAL) and a brass/scintillator hadronic calorimeter (HCAL). An iron/quartz-fiber calorimeter is located in the forward region ($3 < |\eta| < 5$), outside the field volume. Muons are measured with detection planes made of three technologies: Drift Tubes, Cathode Strip Chambers, and Resistive Plate Chambers ($|\eta| < 2.4$).

3 Analysis strategy and simulated samples

The experimental signature in this search is the presence of a high-energy charged lepton and missing transverse energy, $E_{\text{T}}^{\text{miss}}$, which may flag the presence of a non-interacting particle (neutrino). The quantity $\vec{p}_{\text{T}}^{\,\text{miss}}$ is defined as $-\sum \vec{p}_{\text{T}}$ of all reconstructed particles with $E_{\text{T}}^{\text{miss}}$ being the modulus of $\vec{p}_{\text{T}}^{\,\text{miss}}$.

The main discriminant variable used in the search is the transverse invariant mass, M_{T}, defined from the lepton $\vec{p}_{\text{T}}$, the $\vec{p}_{\text{T}}^{\,\text{miss}}$ in the event, and the difference in the azimutal angle between them, as $\text{M}_{\text{T}} = \sqrt{2p_{\text{T}}^{l} E_{\text{T}}^{\text{miss}} (1 - \cos[\Delta\phi(\vec{p}_{\text{T}}^{\,l}, \vec{p}_{\text{T}}^{\,\text{miss}})])}$.

The dominant and irreducible background of this search is $\text{W} \to l\nu$ with $l = \mu, e$. The tau decay channel is also considered as background, although it contributes to the low M_{T} region.

Other background processes are Drell-Yan, where one of the leptons is not reconstructed, $\mathrm{t\bar{t}}$ in their semileptonic or dileptonic decay channel, single top and dibosons, mainly high mass WW (and to a less extent WZ and ZZ). The contribution from these processes is estimated from simulation.

The QCD multijet background, mostly affecting the electron channel, has the largest cross section among all background processes. It is largely rejected by the analysis selection criteria and the remaining contribution to the high mass region is estimated from data. The method, already used in Run-I [3], uses reference regions which are separated from the signal region by using the two uncorrelated quantities serving the kinematic selection, p_{T} and $p_{\mathrm{T}}/\mathrm{MET}$, and the isolation.

The evaluation of the dominant SM W background is achieved using two different samples, one inclusive in mass generated with MADGRAPH 5_aMC@NLO [5] and several exclusive others, covering the boson high mass region, generated with PYTHIA 8.2 [6], tune CUETP8M1 and NNPDF3.0 parton density functions (PDF). A mass-dependent K-factor is calculated, including NNLO QCD using FEWZ 3.2β2 [7] and NLO electroweak corrections using MCSANC 1.01 [8] which provide an accurate description of the tails of the M_{T} distribution, a key element in this search.

High mass Drell-Yan and $\mathrm{t\bar{t}}$ samples, in their semileptonic or dileptonic decays ($\mathrm{t} \to \mu/e$) and in a dedicated high mass bin, m($\mathrm{t\bar{t}}$)>1000 GeV are generated with Powheg [9]. Single top production is generated inclusively with Powheg in the t- and tW-channels and using aMC@NLO in the s-channel. Diboson (WW, WZ and ZZ) production is generated with PYTHIA 8.2, tune CUETP8M1 and CT10 PDF.

Simulation of signal samples (SSM $\mathrm{W}' \to l\nu$) for the electron, muon and tau decay channels, is performed at leading order (LO) with PYTHIA 8.2, Tune CUETP8M1 and using the NNPDF3.0 parton distribution functions. A W′ boson mass dependent K-factor is used to correct for next-to-next-to-leading order (NNLO) QCD cross sections, calculated using FEWZ 3.1β2 [7]. The K-factors vary from 1.3 to 1.1 for the range of W′ masses studied in this analysis, namely from 1.0 to 5.8 TeV. The NNLO corrections decrease with W′-boson masses up to around 4.5 TeV. For higher masses, the K-factor increases and becomes similar to the low-mass values, due to the increased fraction of signal off-shell production.

All generated signal and background events are processed through a full simulation of the CMS detector based on GEANT4 [10], a trigger emulation, and the event reconstruction chain.

The simulation of particle production coming from additional collisions in the same bunch crossing (pileup) is included in all event samples by superimposing minimum bias interactions onto all simulated events.

The analysis is performed in two channels: the $\mathrm{e} + E_{\mathrm{T}}^{\mathrm{miss}}$ and the $\mu + E_{\mathrm{T}}^{\mathrm{miss}}$ channel, where the charged lepton is required to be prompt. Final states where the electron or muon originates from, e.g. a τ decay, are not considered as signal.

4 Object identification and event selection

Candidate events with at least one high-p_{T} lepton are selected using inclusive lepton triggers. Single-muon triggers (with $p_{\mathrm{T}} > 45\,\mathrm{GeV}$ and restricted in muon pseudorapidity, $|\eta| < 2.1$, or $p_{\mathrm{T}} > 50\,\mathrm{GeV}$ and covering the whole pseudorapidity range, $|\eta| < 2.4$), and single-electron ones (with thresholds $E_{\mathrm{T}} > 105$ or 115 GeV) and loose electron identification criteria are used. The

relatively high electron trigger threshold is required in order to suppress non-prompt electrons and jets. The offline reconstructed p_{T} must be greater than 53 (130) GeV in the muon (electron) channel, where the trigger reaches the plateau.

Leptons and $E_{\mathrm{T}}^{\mathrm{miss}}$ are reconstructed using a particle-flow technique [11, 12]. Special requirements which guarantee the presence of good-quality and energetic leptons are applied, optimized for high p_{T} values consistent with the signal region where the analysis is most sensitive. Events containing calorimeter noise or large missing transverse energy due to instrumental effects, such as beam halo or jets near non-functioning channels in the calorimeters, are removed from the analysis.

Electrons are reconstructed from electromagnetic clusters in the ECAL acceptance region (barrel, $|\eta| < 1.444$, endcaps, $1.566 < |\eta| < 2.5$) matched to a track. The identification, optimized for high-p_{T}, includes requirements on isolation and on the shape of the electromagnetic shower. Electron isolation in the tracker is ensured by requiring the p_{T} sum of all tracks within a cone of $\Delta R = \sqrt{(\Delta\phi)^2 + (\Delta\eta)^2} = 0.3$ centered around the track of the electron candidate and originating from the same primary vertex, to be less than 5 GeV. The primary vertex is defined as the vertex with the highest $\sum p_{\mathrm{T}}^2$ in the event, where the sum extends over the associated tracks. The ECAL isolation is defined as the E_{T} sum of the energy deposits within a ΔR= 0.3 cone around the electron candidate, corrected for the mean energy contribution from pileup. The ECAL isolation is required to be below 3% of the electron's E_{T}. The HCAL isolation considers the energy deposits in the hadronic calorimeter within a cone of $\Delta R = 0.15$ around the electron's direction. It must be less than 5% of the electron's energy deposit in the ECAL. In order to differentiate between electrons and photons, properties of the track matched to the calorimeter measurement must be consistent with those of a prompt electron. Specifically, there must be ≤ 1 hit missing in the innermost tracker layers, and the transverse distance to the primary vertex must be $<$0.02 cm (barrel) or $<$0.05 cm (endcap). To reduce the Drell–Yan background, events with additional electrons of $E_{\mathrm{T}} > 35$ GeV are rejected.

For muon reconstruction, information from the inner tracker and the outer muon system are used together. Each muon is required to have at least one hit in the pixel detector, hits in at least four layers of the strip tracker, and segments in two or more muon detector layers. Since consecutive layers are separated by thick layers of steel, the latter requirement significantly reduces the amount of hadronic punch-through. To reduce background from cosmic ray muons, each muon is required to have a transverse impact parameter, $|\mathrm{d_{xy}}| \leq 0.02$ cm and a longitudinal distance parameter, $|\mathrm{d_z}| \leq 0.5$ cm. Both parameters are defined relative to the primary vertex. In order to suppress muons with mismeasured p_{T}, an additional requirement $\sigma_{pT}/p_{\mathrm{T}} < 0.3$ is applied, where σ_{pT} is the uncertainty from the track reconstruction. Muon isolation requires that the scalar p_{T} sum of all tracks originating from the interaction vertex within a $\Delta R = 0.3$ cone around its direction, excluding the muon itself, be less than 10% of the muon's p_{T}. To further reduce the Drell-Yan background the event must not have a second muon with $p_{\mathrm{T}} > 25$ GeV. The muon p_{T} reconstruction is optimized for the high-p_{T} region and its performance has been studied using high-energy cosmic muons and muon pairs from Z decays.

Given the current preliminary detector alignment and in order to ensure a good muon transverse momentum determination, which is the main source of systematic uncertainty affecting the analysis in the muon channel, the pseudorapidity region $|\eta| <$2.0 is used.

Once events containing a high-p_{T} charged lepton are selected, the two-body decay kinematics of the W'$\rightarrow l\nu$ process is exploited for background suppression, applying the following two relatively loose kinematic cuts:

- The difference in azimutal angle between the charged lepton transverse momentum and $\vec{p}_{\mathrm{T}}^{\,\mathrm{miss}}$ is required to be $|\Delta\phi(\vec{p}_{\mathrm{T}}^{\,l}, \vec{p}_{\mathrm{T}}^{\,\mathrm{miss}})| > 2.5$, which ensures a back-to-back configuration between the lepton and $\vec{p}_{\mathrm{T}}^{\,\mathrm{miss}}$.
- The ratio of the charged lepton transverse momentum and $E_{\mathrm{T}}^{\mathrm{miss}}$ must lie in the region $0.4 < p_{\mathrm{T}}/E_{\mathrm{T}}^{\mathrm{miss}} < 1.5$.

Simulated samples, used to account for the contribution of the different background processes, are normalized to the integrated luminosity of the recorded dataset (2.2 fb^{-1}), using calculated NNLO cross sections. The only exception is the diboson sample, for which the NLO cross sections is used. The multijet background in the electron decay channel is estimated from data as in Run-I [3].

5 Systematic uncertainties

Different sources of systematic uncertainties affect this analysis, some of them specific to each decay channel and some others common to both. For each source, its upper/lower value is propagated to the objects' kinematics (e, μ and $E_{\mathrm{T}}^{\mathrm{miss}}$), the resulting distributions are recalculated and the kinematic selection re-applied. The difference in M_{T} distributions with respect to the nominal one is taken as the systematic uncertainty from that source.

In the muon decay channel, the dominant uncertainties come from the possible bias on the momentum scale and the p_{T} resolution. The used simulated samples do not reproduce perfectly the detector performance due to the preliminary knowledge of the alignment of the tracker and muon chambers. Conservative upper values of 0.1/TeV for $|\eta| < 0.9$ and 0.2/TeV for $0.9 < |\eta| < 2.0$ are considered for the p_{T} scale bias and the effect on the muon p_{T} determination taken as a systematic uncertainty. An additional gaussian smearing of 80% of the p_{T} resolution in the simulated samples is taken into account as a systematic uncertainty on the p_{T} resolution. These sources of uncertainty translate directly into the $E_{\mathrm{T}}^{\mathrm{miss}}$ determination, which is mainly given by the high p_{T} lepton and propagate to a 6% (21%) effect on the yields at M_{T} = 1 (2) TeV. The uncertainty on the scale factors derived as the ratio of data to simulation efficiencies for muon triggering and identification are 3%, 5% and 8% for low ($p_{\mathrm{T}} < 500$ GeV), intermediate ($500 < p_{\mathrm{T}} < 1000$ GeV) and high p_{T} regions ($p_{\mathrm{T}} > 1000$ GeV), respectively.

Mismeasurements of the electron energy scale and resolution are typically very small and do not change the M_{T} shape in a sizeable way. The systematic uncertainty in the electron energy scale was estimated to be 1-2% [13] and a conservative 2% is considered. For the electron energy resolution, an additional Gaussian smearing of 2% is applied to the MC simulation. The uncertainties on the electron and positron identification efficiencies when extrapolated to high E_{T} are 4% (6%) in the barrel (endcaps). The estimated uncertainty on the jet energy scale and resolution is translated into the $E_{\mathrm{T}}^{\mathrm{miss}}$ variable. For the Run-II triggers, the efficiencies, SF and uncertainties have been evaluated for the actual single electron trigger used. The uncertainties on the SF (which is consistent with unity) are 0.2% (0.5%) for barrel (endcaps).

Common uncertainties concern the total integrated luminosity (4.6%) and the reweighting procedure applied to simulated samples to exactly match the pileup in data (5%). The application of K-factors accounting for higher-order corrections, both for the signals and the background, is also affected by systematic uncertainties. A flat absolute uncertainty of 5% on the K-factor, stemming from the NNLO coreections, is applied in addition to a M_{T}-dependent uncertainty which derives from the combination of the additive and factorized approaches. The theoretical uncertainty related to the choice of the PDF set is estimated using the updated PDF4LHC prescription [14] and becomes the dominant one at high M_{T} in the electron channel.

6 Results

The transverse mass, M_T, defined in Section 3, is reconstructed for each selected event in data and simulated samples. This is the main discriminant variable used in the analysis, where signal events are expected at very high M_T values, while the different background contributions, and particularly the SM W boson decays appear as a tail as the transverse mass increases, due to the falling cross section. Fig. 1 shows the differential transverse mass (left) and cumulative M_T (right) distributions for the electron channel for $M_T > 200$ GeV. The same distributions are presented for the muon channel in Fig. 2 for values $M_T > 120$ GeV. The increasing bin size at high M_T values in the muon distribution reflects for the muon p_T resolution.

The bottom panels in the M_T distributions present the data over SM prediction ratio, showing good agreement between them within the given uncertainties. For illustration purposes, the expected signal from the decay of two W′ bosons with masses M(W′) = 2.4 and 3.6 TeV are also shown.

Tables 1 and 2 summarize the integrated SM expected number of events compared to data for three representative lower M_T thresholds of 500 GeV, 1 TeV and 1.5 TeV for the electron and muon decay channels, respectively. Also shown is the number of integrated expected signal events for two W′ signal samples of mass M(W′) = 2.4 and 3.6 TeV.

	M_T >500 GeV	M_T >1000 GeV	M_T >1500 GeV
Data	230	11	1.0
SM Background	246 ± 18	14.3 ± 1.2	1.9 ± 0.2
SSM W′ M=2.4TeV	66.1 ± 5.5	58.4 ± 5.2	46.3 ± 4.4
SSM W′ M=3.6TeV	5.5 ± 0.7	4.9 ± 0.7	4.3 ± 0.6

Table 1: Number of events in the electron decay channel integrated above given M_T thresholds of 500, 1000 and 1500 GeV, for data, SM background and two signal examples for M(W′) = 2.4 TeV and 3.6 TeV. The uncertainties given include systematic and statistical uncertainties, except the 4.6% on the total integrated luminosity.

	$M_T > 500$ GeV	$M_T > 1000$ GeV	$M_T > 1500$ GeV
Data	220	10	0
SM Background	251.5 ± 8.8	13.0 ± 1.2	1.8 ± 0.3
SSM W′ M=2.4TeV	94.6 ± 5.2	83.9 ± 4.6	65.8 ± 3.6
SSM W′ M=3.6TeV	6.3 ± 0.3	5.7 ± 0.3	5.0 ± 0.3

Table 2: Number of events in the muon decay channel integrated above given M_T thresholds of 500, 1000 and 1500 GeV, for data, SM background and two signal examples for M(W′) = 2.4 TeV and 3.6 TeV. The uncertainties given include statistical and systematic uncertainties, except the 4.6% on the total integrated luminosity .

The event with the highest mass occurs at M_T ∼2.0 TeV in the electron channel and at M_T ∼1.3 TeV in the muon one.

6.1 Exclusion limits on SSM W′ bosons

As no significant deviation from predictions is seen in the M_T distributions in neither the electron nor the muon decay channels, exclusion limits on new signals are set in the context of the SSM W′ boson production, using the complete M_T distributions for expected background contributions, signals and observed data.

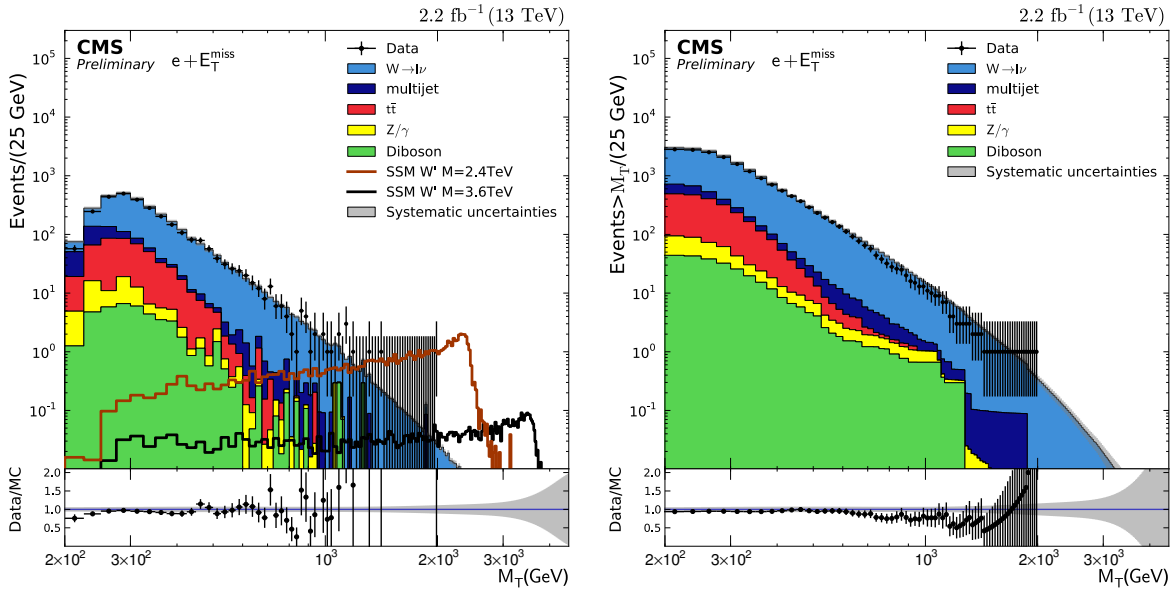

Figure 1: Resulting distributions for data and expected SM backgrounds after kinematic selection in the electron channel: transverse mass M_{T} (left) and M_{T}-cumulative (right). The expected signal from the decay of two W′ bosons with masses M(W′) = 2.4 and 3.6 TeV are also shown. The bottom panels in both figures show the ratio of observed data to SM predictions where the band centered around unity accounts for the systematic uncertainty on the background prediction, without including the 4.6% uncertainty in the luminosity.

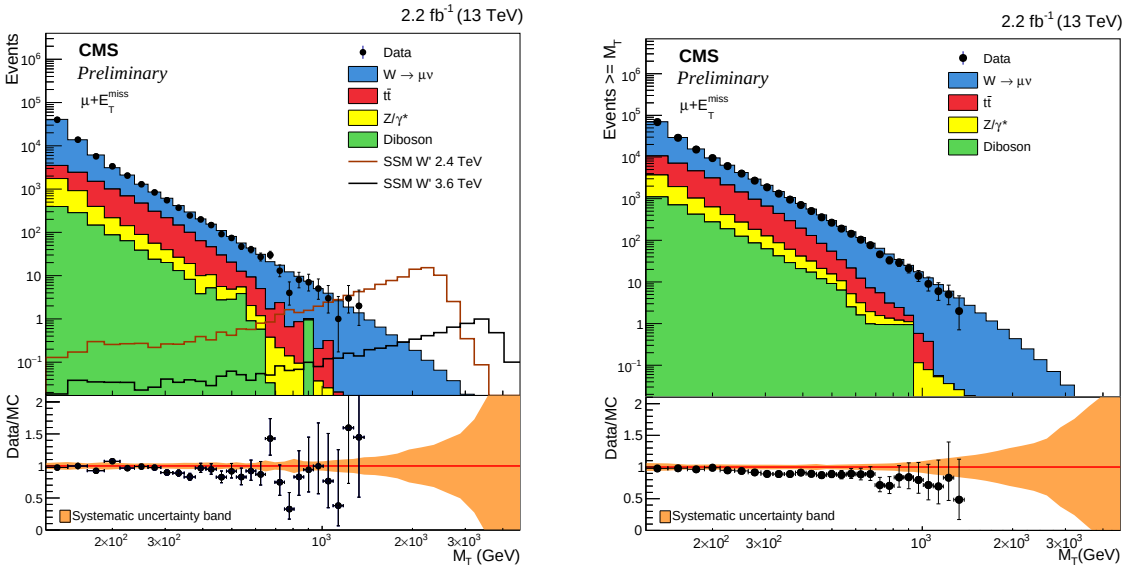

Figure 2: Resulting distributions for data and expected SM backgrounds after kinematic selection in the muon channel: transverse mass M_{T} (left) and M_{T}-cumulative (right). The expected signal from the decay of two W′ bosons with masses M(W′) = 2.4 and 3.6 TeV are also shown. The bottom panels in both figures show the ratio of observed data to SM predictions where the band centered around unity accounts for the systematic uncertainty on the background prediction, without including the 4.6% uncertainty in the luminosity.

Upper limits on the production cross section times branching fraction $\sigma_{W'} \mathcal{B}(W' \to \ell\nu)$, with ℓ = e or μ, are determined using the modified frequentist prescription for the CLs method [15, 16], and asymptotic formulae in the calculation. The limits are computed using a shape analysis both for the expected background processes and signals and the observed data. Systematic uncertainties from Section 5 on the expected signal and background yields are included via nuisance parameters with log-normal prior distributions.

The limits are provided for $M_T > 1$ TeV, where the collected Run-II data are expected to be more sensitive to new physics than the dataset recorded during Run-I, due to the signal cross section dependence with the W′ mass for the concerned center-of-mass energies. Below this M_T value the present analysis of 13 TeV data is not yet as performant as the results from Run-I.

Expected and observed 95% confidence level (CL) limits as a function of W′ mass are shown in Fig. 3, for 2.2 fb^{-1} of data, in the electron (left) and the muon (right) channels. The SSM W′ NNLO cross sections are also depicted as a function of M(W′). The signal acceptance times efficiency, defined as the fraction of simulated signal events passing the event selection, is about 75% for a W′ with mass=3 TeV in both the electron and muon channels. With the present data statistics SSM W′ resonances of masses less than 3.8 TeV (3.8 TeV expected) in the electron channel and 4.0 TeV (3.8 TeV expected) in the muon channel, are excluded at 95 % CL. These results provide tighter limits than the ones obtained from Run-I data.

The combination of both decay channels essentially doubles the statistics and improves the limit such that the production of SSM W′ bosons with masses below 4.4 TeV (4.2 TeV expected) are excluded at 95% CL as shown in Fig. 4.

7 Summary

A search for SSM W′ bosons in final states containing a single high-p_T electron or muon and E_T^{miss}, using 2.2 fb^{-1} of pp collision data at $\sqrt{s}$=13 TeV has been performed. No sign of new physics has been observed and exclusion limits at 95% CL were extracted on the mass of the W′ boson. Masses below 3.8 (4.0) TeV are excluded using the individual electron (muon) decay channels analysis. When both channels are combined the limits on the mass exclusion extend to 4.4 TeV. These values significantly improve the results obtained with the Run-I collected data.

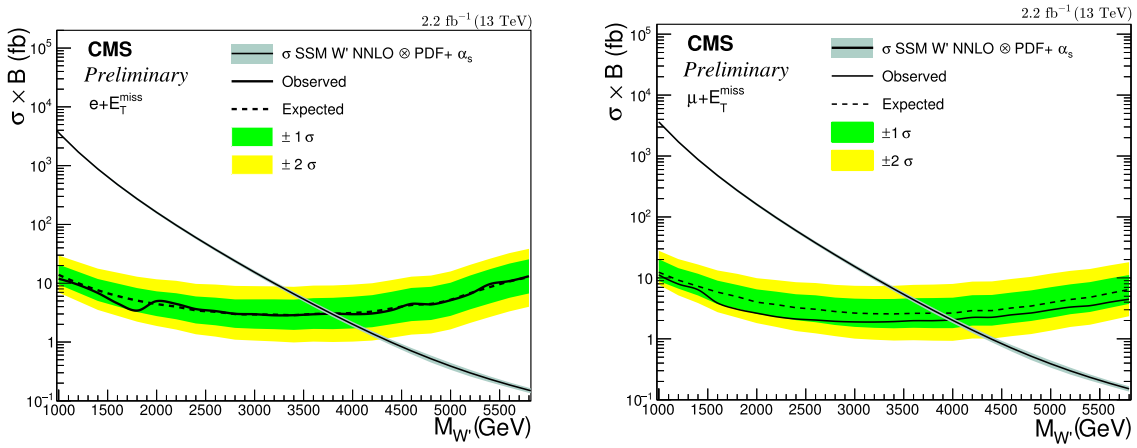

Figure 3: Expected and observed 95% CL limits for the electron (left) and muon (right) channels. The expected(observed) limit are displayed as a dashed(solid) line and the green(yellow) bands represent the one(two) sigma uncertainty bands. The SSM W′ NNLO cross sections are depicted as a function of M(W′).

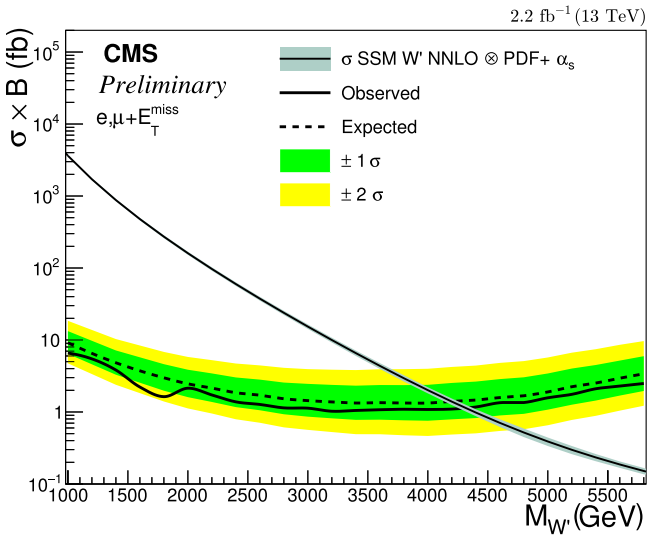

Figure 4: Expected and observed 95% CL limits for the combination of the electron and muon channels. The expected(observed) limit are displayed as a dashed(solid) line and the green(yellow) bands represent the one(two) sigma uncertainty bands. The SSM W′ NNLO cross sections are depicted as a function of M(W′).

References

[1] G. Altarelli, B. Mele, and M. Ruiz-Altaba, "Searching for new heavy vector bosons in $p\bar{p}$ colliders", *Z. Phys. C* **45** (1989) 109, doi:10.1007/BF01556677.

[2] G. Aad et al., "Search for new particles in events with one lepton and missing transverse momentum in pp collisions at $\sqrt{(s)}$ = 8 TeV with the ATLAS detector", *JHEP* **2014** (2014), no. 9, doi:10.1007/JHEP09(2014)037.

[3] CMS Collaboration, "Search for physics beyond the standard model in final states with a lepton and missing transverse energy in proton-proton collisions at $\sqrt{(s)}$ = 8 TeV", *Phys. Rev.* **D91** (2015), no. 9, 092005, doi:10.1103/PhysRevD.91.092005, arXiv:1408.2745.

[4] CMS Collaboration, "The CMS experiment at the CERN LHC", *JINST* **3** (2008) S08004, doi:10.1088/1748-0221/3/08/S08004.

[5] J. Alwall et al., "The automated computation of tree-level and next-to-leading order differential cross sections, and their matching to parton shower simulations", *JHEP* **07** (2014) 079, doi:10.1007/JHEP07(2014)079, arXiv:1405.0301.

[6] T. Sjöstrand, S. Mrenna, and P. Skands, "PYTHIA 6.4 physics and manual", *JHEP* **05** (2006) 026, doi:10.1088/1126-6708/2006/05/026, arXiv:hep-ph/0603175.

[7] R. Gavin, Y. Li, F. Petriello, and S. Quackenbush, "W Physics at the LHC with FEWZ 2.1", *Comput. Phys. Commun.* **184** (2013) 208–214, doi:10.1016/j.cpc.2012.09.005, arXiv:1201.5896.

[8] S. G. Bondarenko and A. A. Sapronov, "NLO EW and QCD proton-proton cross section calculations with mcsanc-v1.01", *Comput.Phys.Commun.* **184** (2013) 2343–2350, doi:10.1016/j.cpc.2013.05.010, arXiv:1301.3687.

[9] L. Barze et al., "Neutral current Drell-Yan with combined QCD and electroweak corrections in the POWHEG BOX", *Eur. Phys. J.* **C73** (2013), no. 6, 2474, doi:10.1140/epjc/s10052-013-2474-y, arXiv:1302.4606.

[10] GEANT4 Collaboration, "GEANT4: A Simulation toolkit", *Nucl. Instrum. Meth.* **A506** (2003) 250–303, doi:10.1016/S0168-9002(03)01368-8.

[11] CMS Collaboration, "Particle–flow event reconstruction in CMS and performance for jets, taus, and $E_{\mathrm{T}}^{\mathrm{miss}}$", CMS Physics Analysis Summary CMS-PAS-PFT-09-001, 2009.

[12] CMS Collaboration, "Commissioning of the particle-flow event reconstruction with the first LHC collisions recorded in the CMS detector", CMS Physics Analysis Summary CMS-PAS-PFT-10-011, 2010.

[13] Z. group, "Search for High-Mass Resonances Decaying to Muon or Electron Pairs at $\sqrt{s} = 13$ TeV", *CMS Physics Analysis Summary CMS-PAS-EXO-15-005* (2015).

[14] J. Butterworth et al., "PDF4LHC recommendations for LHC Run II", arXiv:1510.03865.

[15] A. L. Read, "Presentation of search results: the CL s technique", *J. Phys. G: Nucl. Part. Phys.* **28** (2002), no. 10, 2693.

[16] T. Junk, "Confidence level computation for combining searches with small statistics", *Nucl. Instrum. Meth.A* **434** (1999), no. 2-3, 435 – 443, doi:doi:10.1016/S0168-9002(99)00498-2.